Ninth Canadian Conference on
Earthquake Engineering
Ottawa, Ontario, Canada
26-29 June 2007

SEISMIC RESPONSE OF RC COLUMNS WITH STRENGTH DETERIORATION

B. Acun[1] and H. Sucuoglu[2]

ABSTRACT

Preliminary results of a developing study are presented in this paper. In the analytical part, a hysteresis model is proposed for deteriorating concrete components under seismic action. The shape of the hysteresis loops are controlled by the dissipated cumulative energy whereas the ultimate strength is governed by the low cycle fatigue behavior. These two basic parameters are obtained experimentally from full scale specimens tested under constant amplitude displacement cycles. The first phase of the experimental program presented herein constitutes from sub standard column specimens, representing poor existing concrete structures. The second phase of testing will be conducted on standard quality reinforced concrete columns.

Introduction

Severe seismic events in urban regions during the last two decades revealed that the structures constructed before the development of modern seismic codes are the most vulnerable to earthquakes. Sub standard reinforced concrete buildings constitute an important part of this highly vulnerable urban building stock. There is urgent need for the development and improvement of methods for seismic performance assessment of existing reinforced concrete structures. Several researchers proposed different evaluation techniques in the past for performance assessment of concrete structures, either by using global structural response parameters, or by quantifying the structural member performances (Stephens and Yao 1987, McCabe and Hall 1989, Williams and Sexsmith 1995, Ghobarah et al. 1999). As an alternative to these conventional methods, the preliminaries of a performance evaluation procedure for structural members, mainly columns, by using an energy-based approach combined with low cycle fatigue concept is proposed in this study. The basic aim is to develop an energy-based hysteresis model for reinforced concrete columns incorporating deterioration behavior under repeated displacement cycles. Although there are previous experimental works conducted on the effect of loading history on seismic response of R/C members (Hwang Scribner 1984, El-Bahy et al. 1999), the proposed energy-based hysteresis model particularly employs dissipated energy as the basic parameter controlling the shape of hysteresis loops. Cyclic degradation in strength is another independent control parameter which is obtained experimentally from the low cycle fatigue behavior of reinforced concrete.

[1]Research Assistant, Dept. of Civil Engineering, Kocaeli University, Kocaeli, Turkey (Currently on leave at Middle East Technical University for graduate study)
[2]Professor, Dept. of Civil Engineering, Middle East Technical University, Ankara, Turkey

Experimental Program

A two-phase experimental program on full-scale columns has been initiated. Testing of seven sub standard specimens, with plain bars and low concrete strength (~13 MPa), were planned in the first phase. These specimens represent the columns of existing buildings constructed before 70's in Turkey with poor detailing and low concrete strength. The aim of this phase was to obtain information on the deterioration behavior of such structural components. In the second phase of the program, testing of another seven specimens with deformed bars and proper detailing is programmed. The concrete strength for the second set of specimens was selected as 25 MPa. This set represents the columns designed and detailed according to the current Seismic Code (1998) of Turkey. Only the results of first five columns from the first phase are presented and discussed in this paper. Amplitude of the imposed tip displacement was employed as the basic testing variable.

Test Specimens

The columns had 350 mm square cross-section and their clear height was 1800 mm. They were cast with rigid footings vertically in order to represent the actual casting in building construction. Footings had dimensions of 1350x500x400 mm and they were properly reinforced.

As it was the case in most of the existing concrete buildings in Turkey constructed before 70's, plain bars were used as longitudinal and transverse reinforcements in column specimens. All five columns were longitudinally reinforced with eight ϕ 14 plain bars (ρ_l = 1%) and transversely reinforced with ϕ 8 hoops and ties. A peripheral hoop with 90° hooks and a pair of cross ties with 135° hook at one end and 90° hook at the other hand were used as the set of transverse reinforcement at one layer. The transverse bar sets were spaced at 165 mm, from the bottom of column through the 4/5 of the clear height. The spacing was then reduced to 50 mm at the top part of the columns where stress concentration was expected due to lateral and axial loading. Dimensional and reinforcement details of a typical specimen are shown in Fig. 1, and these details are summarized in Table 1 along with the material properties of specimens.

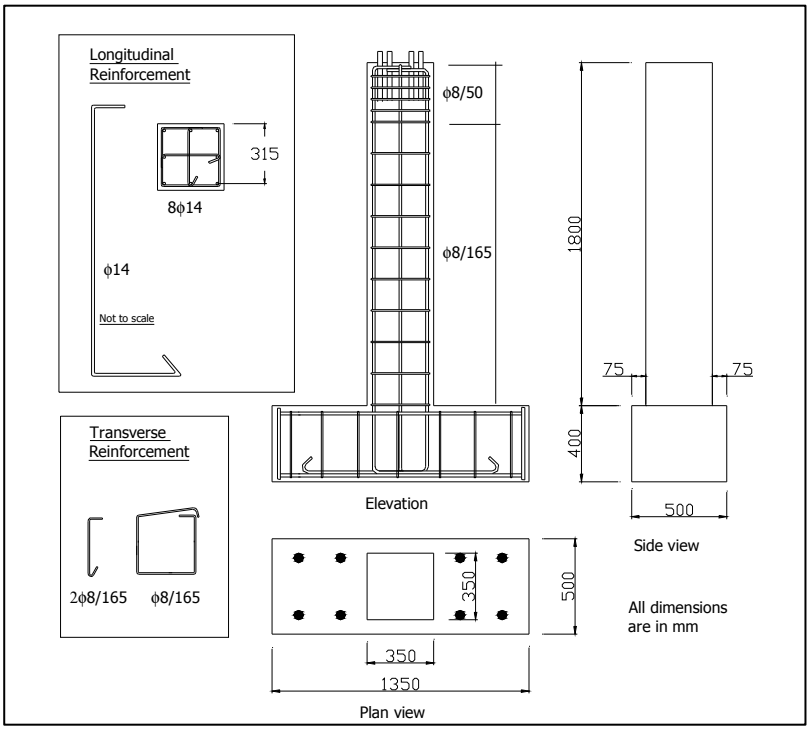

Figure 1. Dimensions and details of a typical specimen.

Table 1. Material properties of test specimens.

Test Specimen	f'_c	Longitudinal Reinforcement (8ϕ14)			Transverse Reinforcement (ϕ8/165)			Axial Load Ratio
		Yield Strength	Ultimate Strength	Ratio	Yield Strength	Ultimate Strength	Vol. Ratio	$N / A_g f_c$
	(MPa)	(MPa)	(MPa)	(%)	(MPa)	(MPa)	(%)	
CP12	13.5	315	448	1.00	368	487	0.57	~0.2
CP24	12.4							
CP33_u	13.2							
CP43	12.2							
CP56	11.4							

The only test parameter was the imposed tip displacement. All specimens were constructed with identical dimensions and reinforcement detailing, except the specimen CP33_u. In specimen CP33_u, the longitudinal bars were covered with a thin layer of silicone and rubbed with grease from the level of column-footing intersection to the top of column (except the hooks at the upper end of the column) in order to reduce/prevent the bond between longitudinal bars and concrete.

A simple notation was used for the designation of test specimens. The first two characters of the specimen names represent the bar type used as longitudinal reinforcement in specimens. The third character indicates the number of specimen. The fourth character indicates the amplitude of imposed tip displacement in the first constant stage of loading history in terms of ductility, and the last character after underscore, if any exists, indicates the state of exception. Hence the specimen name CP33_u indicates a column specimen with plain bars, tested as the third specimen, under constant amplitude tip displacement cycles (in the first stage of loading) of $\mu = 3$ and the bond between longitudinal bars and concrete were prevented as the exception.

Test Setup and Instrumentation

Specimens were placed and tested on a mat foundation, fixed to the strong floor with post tensioned bars. A steel head was placed on top of the columns and lateral load was applied by an actuator with hinges attached at both ends, from the level of this steel head. Two steel beams were placed on either side of the specimen parallel to the loading direction and a set of rollers were attached to the upper part of columns in order to prevent the out-of-plane movement of specimens.

Axial load was applied by a steel loading beam placed horizontally on the steel head, perpendicular to the loading direction. Two high strength steel rods with hinges at footing level were connected both to the steel loading beam and mat foundation and load was applied by post-tensioning of these rods. Axial load level was kept nearly constant during the tests. The general view of test setup is shown in Fig. 2.

The applied loads (lateral and axial) were measured by using calibrated load cells. The response of test specimen was measured with LVDT's placed at several levels of each specimen. Four dial gages were mounted on both sides of each column at 350 mm level from the top of the specimen footing. Sixteen strain gages (12 at longitudinal bars, 4 at stirrups) were installed on each specimen. Nominal locations of instruments are shown in Fig. 3.

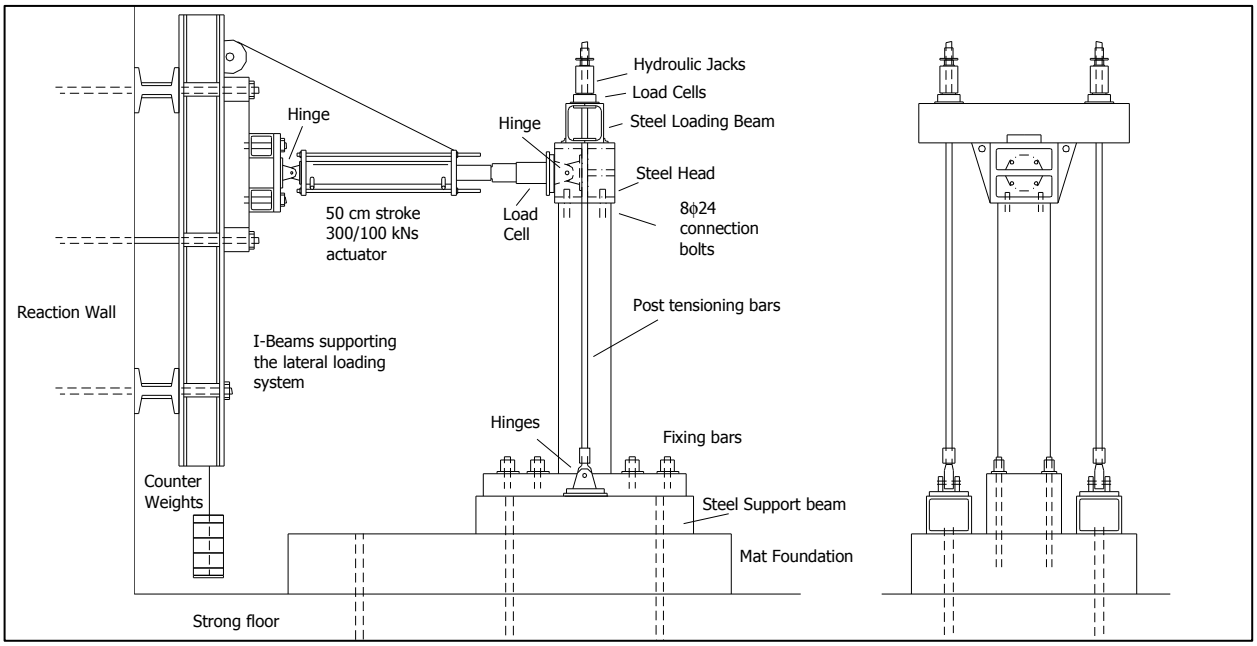

Figure 2. General view of test setup.

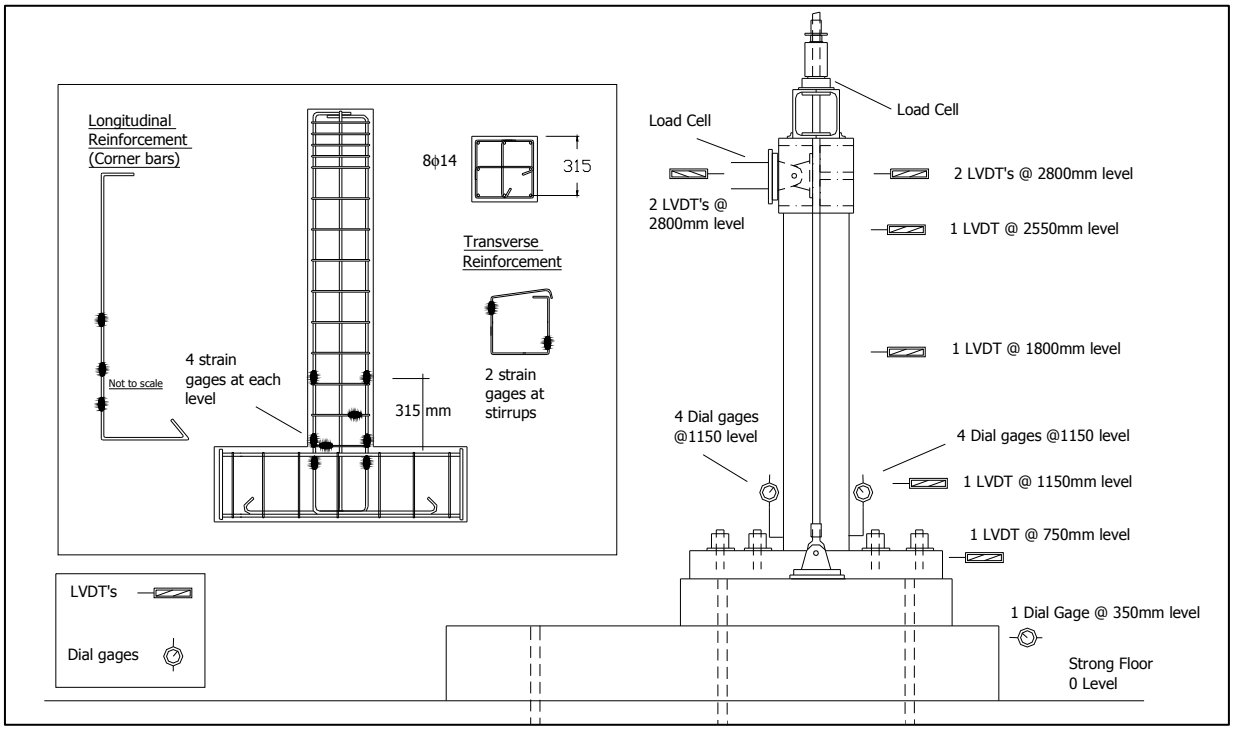

Figure 3. Instrumentation and strain gage locations of test specimen.

Testing Program

All tests were started with the application of constant axial load on specimens. When the desired axial load level was attained, it was kept constant and lateral load application procedure was initiated.

Specimens were tested under displacement controlled loadings. Two-staged constant amplitude cyclic displacement patterns were imposed on the specimens. Specimen CP12 was tested under 35 mm displacement cycles in the first stage of loading, then the displacement amplitude was increased to 70 mm. Specimen CP24 was tested under 70 mm displacement cycles at the initial stage. The amplitude then increased to 105 mm. For specimen CP33_u and specimen CP43 same loading history was applied. At the first stage, 50 mm displacement cycles were imposed on both specimens. In the second stage, the amplitude was increased to 70 mm. At the end of the second stage, testing was continued with 150 mm displacement cycles for specimen CP33_u and with 105 mm displacement cycles for specimen CP43, in order to observe the failure modes of the specimens. The fifth specimen, CP56 was tested under 105 mm displacement cycles initially and then the amplitude of cycles were reduced to 70 mm. Imposed displacement histories for all specimens are shown in Fig. 4.

During the tests, behavior of specimens was monitored continuously with installed instruments and information concerning cracking and crushing of concrete, buckling of long bars, etc. was recorded.

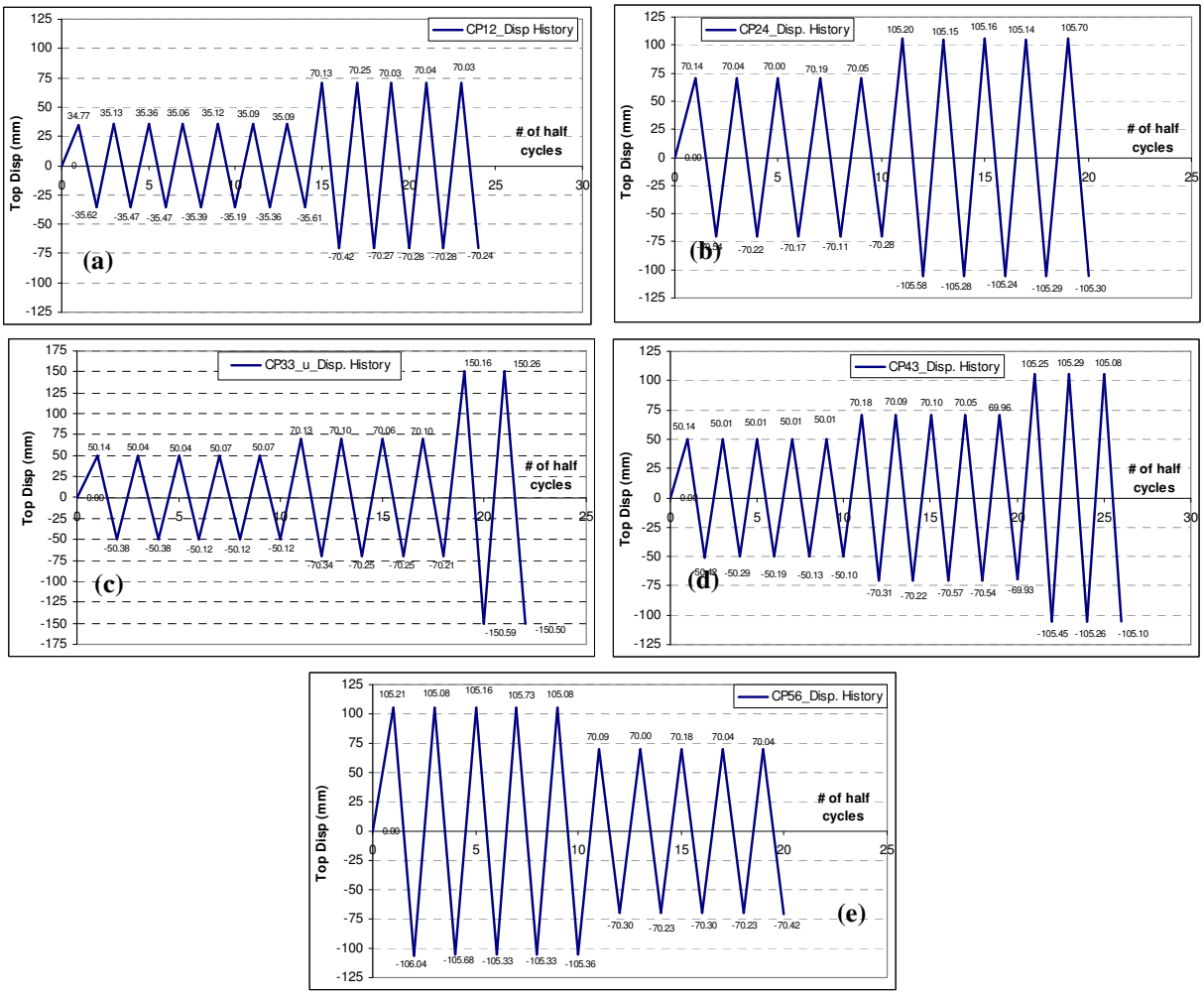

Figure 4. Imposed displacement histories of specimens; (a) CP12, (b) CP24, (c) CP33_u, (d) CP43, (e) CP56.

Experimental Results

General Behavior

The lateral load – tip displacement hysteresis loops are presented in Fig. 5. Lateral load measured from the load cell is corrected for the P-Δ effect caused by geometric nonlinearity of the loading system. All specimens except CP33_u were identical. However they were subjected to different cyclic displacement histories in order to observe the low cycle fatigue effect on strength and energy dissipation capacity. CP33_u was unbonded, and it was subjected to the same displacement history with CP43. The envelope curves of positive half cycles for the force - displacement responses of all specimens are also plotted in Fig. 5.f.

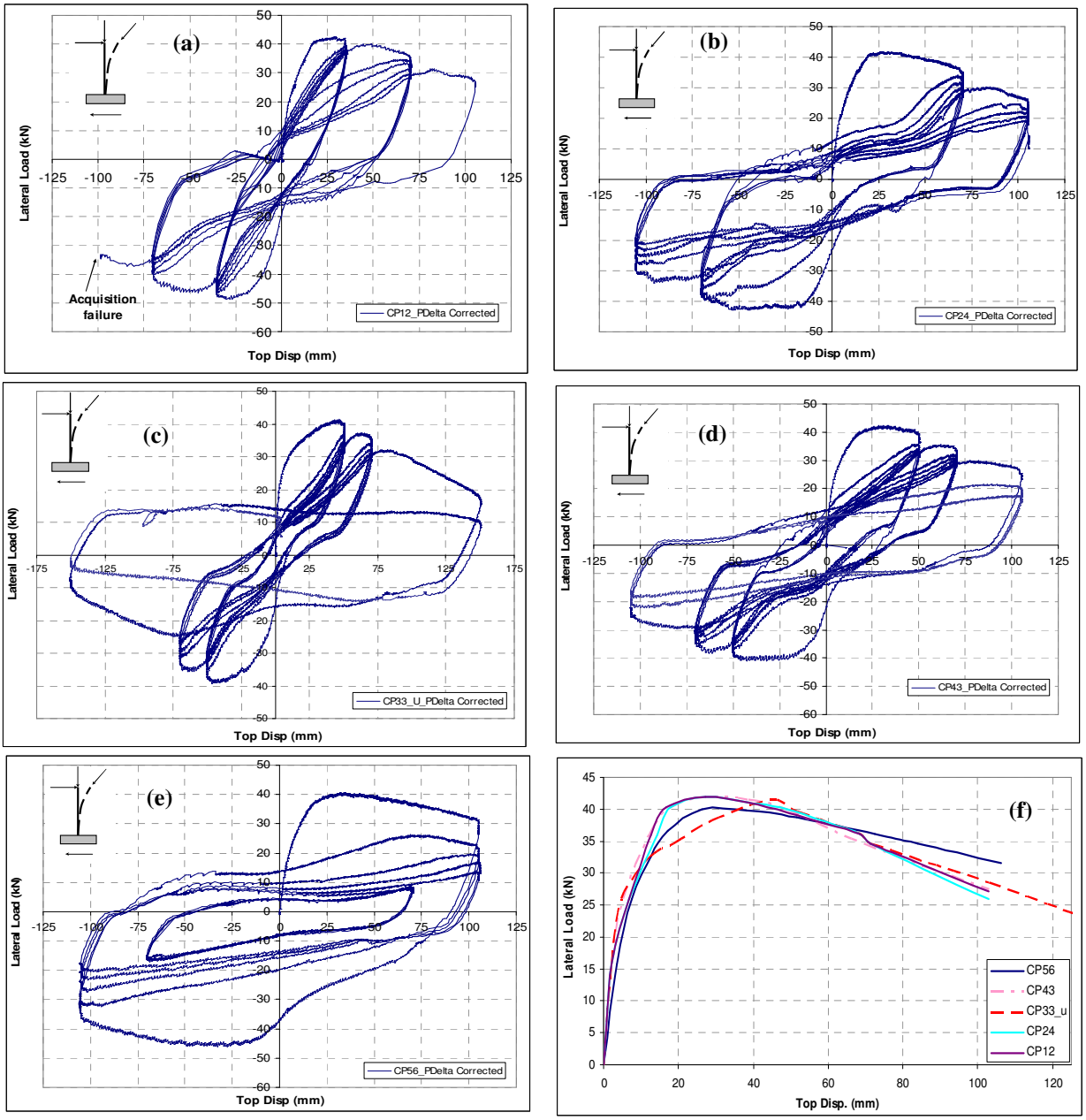

Figure 5. Lateral load versus tip displacement curves (P-Δ corrected) of specimens (a) CP12, (b) CP24, (c) CP33_u, (d) CP43, (e) CP56 and (f) envelope curves for positive half cycles of all specimens.

All specimens failed in the flexure dominated failure mode. In all five tests, first flexural cracks were developed in regions close to the column base - footing intersection zones. Except Specimen CP33_u, the cracks on each specimen were then spread along the column height, but the width of these cracks remained minor till the end of imposed loading histories while the width of cracks at the base region increased. In Specimen CP33_u, a single crack was developed at the base region of specimen, typical for an unbonded member, and this crack was widened at the later stages of loading program while only the hairline cracks were observed along the column height. A plastic hinging zone formed at about a height of h/2 (≈ 170 mm) from the bottom end of all column specimens which actually corresponds nearly the level of first transverse reinforcement set. Testing has ended with the buckling of column longitudinal reinforcement.

Cumulative Dissipated Energy

Cumulative dissipated energy curves of each test specimen for all loading histories are presented in Fig. 6. It can be seen from Fig's 4.b and 4.e that the specimens CP24 and CP56 were subjected to the same amplitudes of loading, but with different sequences, in order to observe the affect of loading patterns on energy dissipation characteristics. Although the observed experimental behaviors were quite different due to sequence of imposed displacements, both specimens dissipated nearly the same amount of energy cumulatively at the end of tests, which might be an indication of path independency in terms of cumulative dissipated energy. It is expected to derive a more accurate statement on path dependency after the conclusion of full testing program with the evaluation of variable amplitude test results.

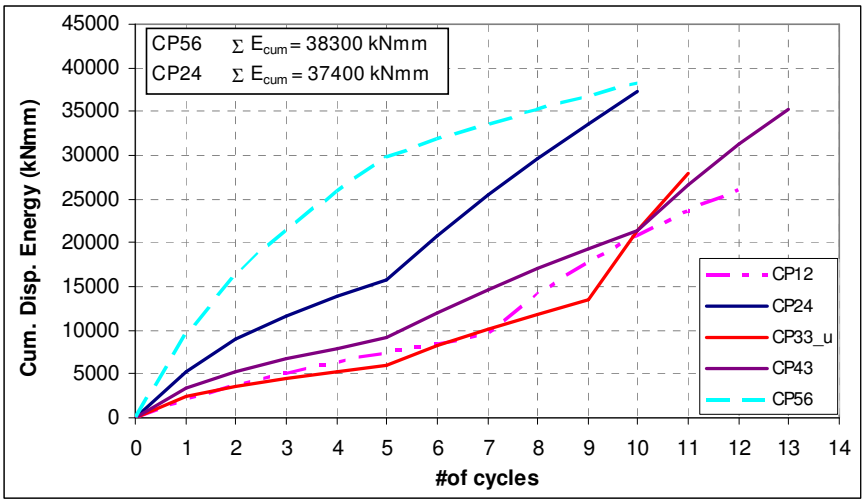

Figure 6. Cumulative dissipated energy per cycle curves of test specimens.

Energy and Strength Degradation

Considering only the first constant-amplitude stages of all tests (i.e. the first 5 full cycles, including CP43), typical energy degradation curves of each specimen are constructed by normalizing the dissipated energies of each full cycle with respect to the energy dissipated at the first full cycle of that specimen. These energy degradation curves are plotted in Fig. 7. Although degradation curve of Specimen CP12 exhibits a slightly different variation, all curves tend to form a bundle which indicates that the energy degradation of identical specimens may be independent from the imposed displacement amplitude.

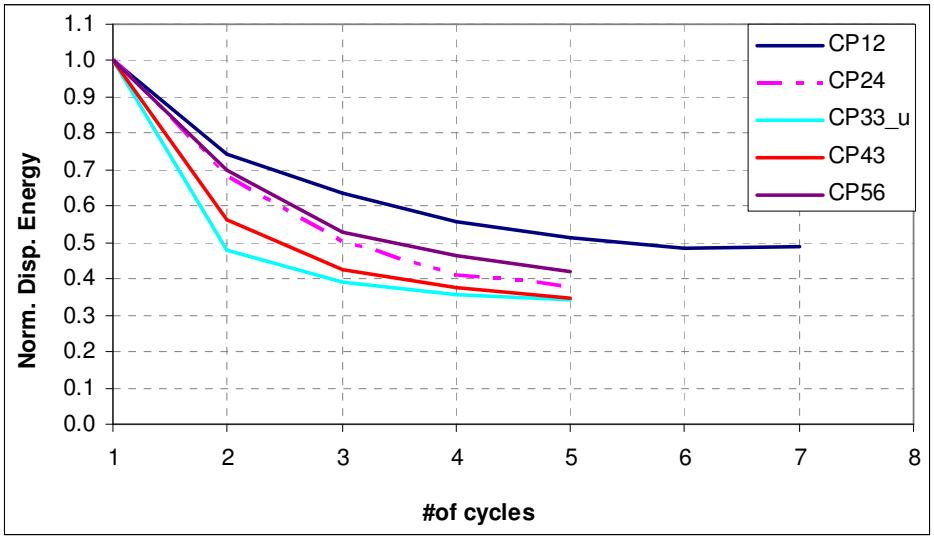

Figure 7. Normalized dissipated energy curves of test specimens.

Employing the same idea, curves of strength degradation at attained maximum tip displacement in the first constant-amplitude stage of loading history are plotted in Fig. 8 for positive and negative half cycles for each specimen, respectively. Strength values of each half cycle at the maximum attained displacement are normalized with respect to the corresponding strength value of the first positive or negative half cycle of that specimen, respectively. It can be observed that the normalized cyclic strength degradation with low cycle fatigue is also independent of displacement amplitude, except the specimen CP56. This specimen was subjected to a constant ductility of approximately 6, which was apparently beyond its capacity of maintaining stable strength under low cycle fatigue loading.

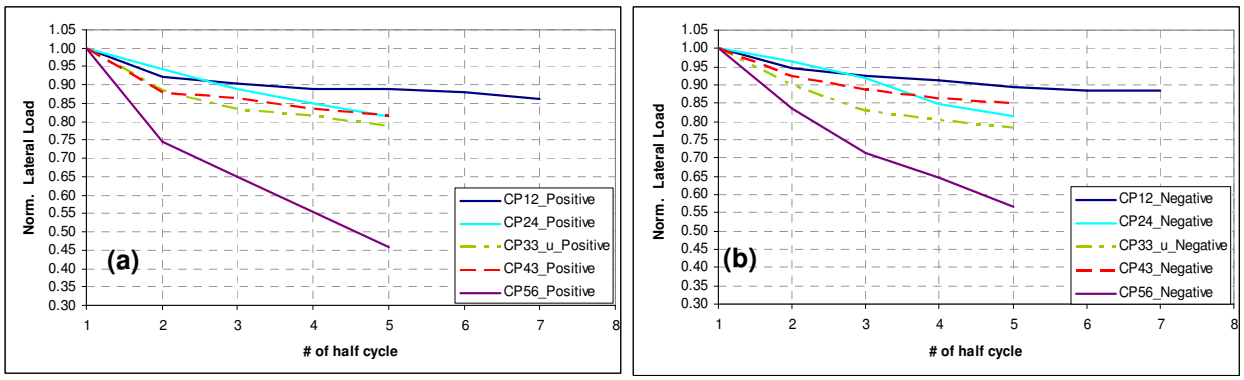

Figure 8. Strength degradation curves of specimens at maximum attained tip displacement for (a) positive and (b) negative half cycles.

Analytical Prediction

A preliminary study on an energy based hysteresis model is initiated by employing typical energy degradation and strength degradation curves from experimental results of R/C column specimens with properties given in the previous sections. A formulation with the general form given in Eq. 1 was derived for prediction of hysteresis loops with the known boundary conditions (maximum displacement of a half-cycle, strength at maximum displacement of that half-cycle, energy dissipated in that half-cycle).

$$\underline{\mathbf{C}}\,\underline{\mathbf{a}} = \underline{\mathbf{B}} \qquad (1)$$

Here, $\underline{\mathbf{a}}$ is the vector of three unknown coefficients for a quadratic re-loading hysteresis curve. $\underline{\mathbf{C}}$ and $\underline{\mathbf{B}}$ are the functions of strength, displacement amplitude and energy dissipated during that half-cycle.

Balancing the dissipated energy of any typical experimental cycle with energy from the corresponding analytical cycle, hysteresis loops are constructed. For unloading stiffness of hysteresis loops, the linear formulation proposed by Takeda et al. (1970) was utilized.

Cycle-by-cycle matches on the experimental loops of Specimen CP24 are presented in Fig. 9 as an example of the analytical prediction of hysteresis loops.

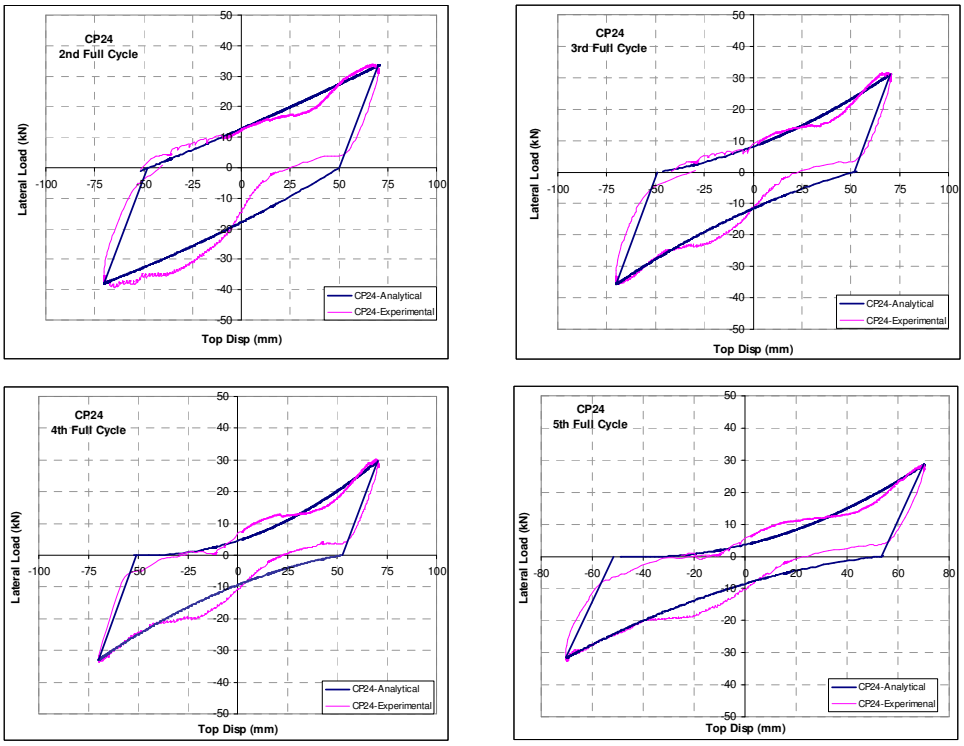

Figure 9. Measured and calculated hysteresis loops for Specimen CP24.

Discussion of Results

Common characteristics of deteriorating structural components which are exhibited by the load-deflection relationships are degradation in strength and stiffness under displacement reversals imposed by seismic excitation. Degradation in flexural strength is perhaps related to the reduction of moment arm in the plastic section due to shifting of concrete stress block, and degradation in stiffness is related to pinching due to primarily bond slip. Several hysteresis relations had been proposed in the past, from simple (Clough and Johnston, 1966) to sophisticated (Takeda et al., 1970) for predicting the flexural deterioration behavior of reinforced concrete under repeated loading. More sophisticated models are present for modeling bond slip. Despite analytical sophistication to various levels, a wiggle by wiggle match is impossible to obtain because of the inherent randomness in reinforced concrete behavior. The approach taken in this study is different in the general sense. If the degradation in strength and energy dissipation capacity can be predicted from constant-amplitude low cycle fatigue experiments, then simple but accurate representation of hysteretic behavior can be obtained. It is demonstrated in this presentation that this is possible under

constant-amplitude displacement cycles. Sucuoğlu and Erberik (2004) showed that this is also possible under variable amplitude displacements. The remaining task is to categorize the degradation of strength and energy dissipation capacity under low cycle fatigue with the general characteristics of reinforced concrete members. Conformance (and non conformance) to modern seismic code detailing rules is proposed as the two basic classes for the investigation in progress.

References

Clough, R. W. and Johnston, S. B.,1966. Effect of stiffness degradation on earthquake ductility requirements. *Proceedings, Second Japan National Conference on Earthquake Engineering*, 227-232

El-Bahy, A., Kunnath, S. K., Stone, W. C., Taylor, A. W., 1999. Cumulative Seismic Damage of Circular Bridge Columns: Benchmark and Low-Cycle Fatigue Tests, *ACI Structural Journal,* 96-S71, 633-641.

Ghobarah, A., Aziz, T. and Abou-Elfath, H., 1999. Softening effects on seismic response of non-ductile concrete frames, *Journal of Earthquake Engineering*, 3, (1), 59-81.

Hwang, F. H. and Scribner, C. F., 1984. RC Member Cyclic Response During Various Loading, *Journal of Structural Engineering, ASCE,*110 (3), 466-489.

McCabe, S. L. and Hall, W. J., 1989. Assessment of seismic structural damage, *Journal of Structural Engineering, ASCE*, 115, (9), 2166-2183.

Stephens, J. E. and Yao, J. T. P., 1987. Damage assessment using response measurements, *Journal of Structural Engineering*, ASCE 113(4), 787–801

Sucuoğlu, H. and Erberik, A., 2004. Energy-based hysteresis and damage models for deteriorating systems. *Earthquake Engineering and Structural Dynamics,* 33. 69-88.

Takeda, T., Sozen, M., Nielsen, N., 1970. Reinforced concrete response to simulated earthquakes, *Journal of the Structural Division, ASCE,* 96 (12), 2557-2573

Williams, M. S. and Sexsmith, R. G., 1995. Seismic damage indices for concrete structures: A State-of-the-Art Review, *Earthquake Spectra*, 11, (2), 319-349.